Nuclear structure in the Quark-Meson Coupling (QMC) model

K. Martinez-Paglinawan

A.W. Thomas, J.R. Stone, P. A. M. Guichon

September 5, 2022

Motivation

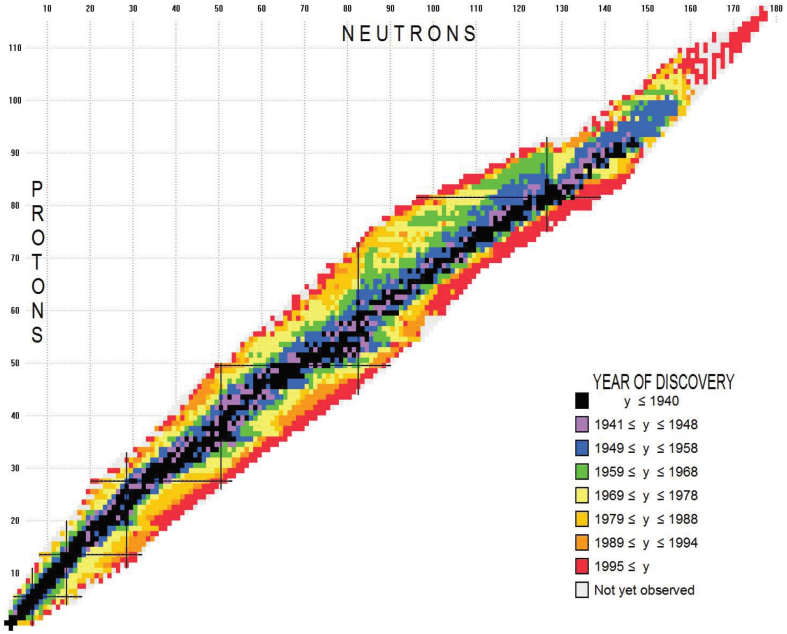

Figure from NuBASE 2017, AME 2016

Motivation

PRL 116, 092501 (2016) PHYSICAL REVIEW LETTERS week ending 4 MARCH 2016

Finite Nuclei in the Quark-Meson Coupling Model

J. R. Stone,[1,2] P. A. M. Guichon,[3] P. G. Reinhard,[4] and A. W. Thomas[5]
[1]*Department of Physics, University of Oxford, Oxford OX1 3PU, United Kingdom*
[2]*Department of Physics and Astronomy, University of Tennessee, Knoxville, Tennessee 37996, USA*
[3]*SPhN-IRFU, CEA Saclay, F91191 Gif sur Yvette, France*
[4]*Institut für Theoretische Physik II, Universität Erlangen, D-91058 Erlangen, Germany*
[5]*ARC Centre of Excellence in Particle Physics at the Terascale and CSSM, Department of Physics, University of Adelaide, SA 5005 Australia*
(Received 8 August 2015; published 29 February 2016)

We report the first use of the effective quark-meson coupling (QMC) energy density functional (EDF), derived from a quark model of hadron structure, to study a broad range of ground state properties of even-even nuclei across the periodic table in the nonrelativistic Hartree-Fock + BCS framework. The novelty of the QMC model is that the nuclear medium effects are treated through modification of the internal structure of the nucleon. The density dependence is *microscopically* derived and the spin-orbit term arises naturally. The QMC EDF depends on a single set of four adjustable parameters having a clear physics basis. When applied to diverse ground state data the QMC EDF already produces, in its present simple form, overall agreement with experiment of a quality comparable to a representative Skyrme EDF. There exist, however, multiple Skyrme parameter sets, frequently tailored to describe selected nuclear phenomena. The QMC EDF set of fewer parameters, derived in this work, is not open to such variation, chosen set being applied, without adjustment, to both the properties of finite nuclei and nuclear matter.

DOI: 10.1103/PhysRevLett.116.092501

Motivation

- A description of NN interaction starting from quarks that can be employed for nuclear systems across the nuclear chart

Motivation

- A description of NN interaction starting from quarks that can be employed for nuclear systems across the nuclear chart
- The Quark–Meson–Coupling (QMC) model self-consistently relates the dynamics of the internal quark structure of a hadron to the relativistic mean fields arising in nuclear matter

Motivation

- A description of NN interaction starting from quarks that can be employed for nuclear systems across the nuclear chart
- The Quark–Meson–Coupling (QMC) model self-consistently relates the dynamics of the internal quark structure of a hadron to the relativistic mean fields arising in nuclear matter
- The QMC model energy density functional (EDF) was successfully employed to investigate several ground state properties of even-even finite nuclei across the nuclear chart

Motivation

- A description of NN interaction starting from quarks that can be employed for nuclear systems across the nuclear chart
- The Quark–Meson–Coupling (QMC) model self-consistently relates the dynamics of the internal quark structure of a hadron to the relativistic mean fields arising in nuclear matter
- The QMC model energy density functional (EDF) was successfully employed to investigate several ground state properties of even-even finite nuclei across the nuclear chart
- A derivative-free optimization procedure (POUNDerS) is available to use to optimize nuclear EDFs

Motivation

- A description of NN interaction starting from quarks that can be employed for nuclear systems across the nuclear chart
- The Quark–Meson–Coupling (QMC) model self-consistently relates the dynamics of the internal quark structure of a hadron to the relativistic mean fields arising in nuclear matter
- The QMC model energy density functional (EDF) was successfully employed to investigate several ground state properties of even-even finite nuclei across the nuclear chart
- A derivative-free optimization procedure (POUNDerS) is available to use to optimize nuclear EDFs
- Several nuclear observables are left to be studied using the QMC model and further development in the model is sought for better predictions of such observables

Motivation

- K. L. Martinez, A. W. Thomas, J. R. Stone, and P. A. M. Guichon. "Parameter optimization for the latest quark-meson coupling energy-density functional". In: *Phys. Rev.* C 100 (2019), p. 024333. DOI : 10.1103/PhysRevC.100.024333.
- K. L. Martinez, A. W. Thomas, P. A. M. Guichon, and J. R. Stone. "Tensor and pairing interactions within the quark-meson coupling energy-density functional". In: *Phys. Rev.* C 102 (2020), p. 034304. DOI : 10.1103/PhysRevC.102.034304.
- S. Antić, J. R. Stone, J. C. Miller, K. M. L. Martinez, A. W. Thomas and P. A. M. Guichon. "The outer crust of a cold, non-accreting neutron star within the Quark-Meson Coupling (QMC) model". arXiv:2006.16521 [nucl-th].

The QMC Model

The QMC Model

- employs relativistic mean-field theory

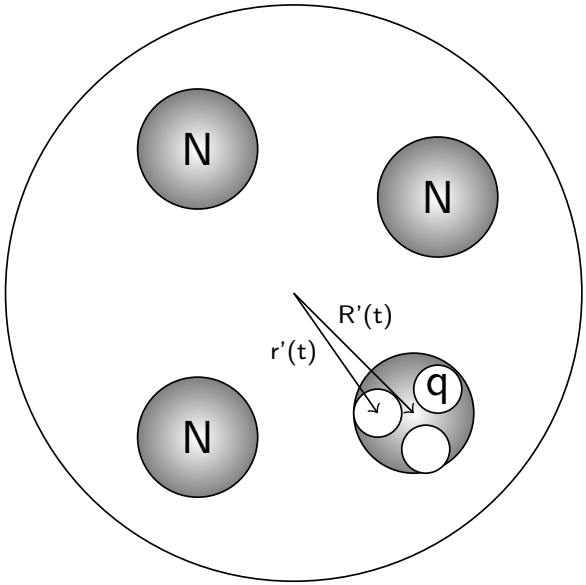

The QMC Model

- employs relativistic mean-field theory
- utilises the MIT bag model of a nucleon; assumes that nucleon bags do not overlap

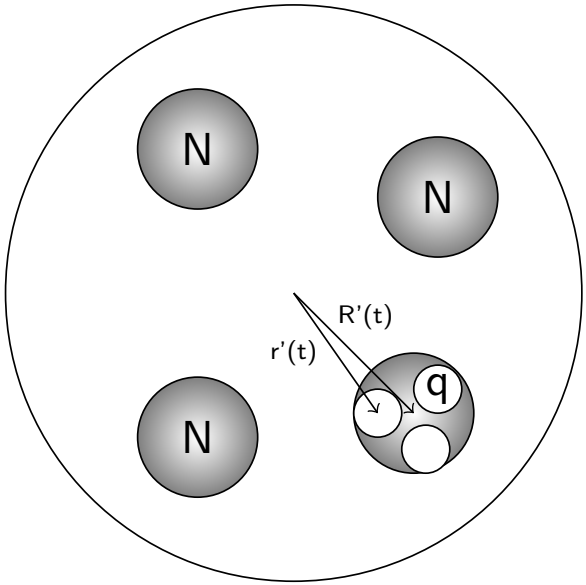

The QMC Model

- employs relativistic mean-field theory
- utilises the MIT bag model of a nucleon; assumes that nucleon bags do not overlap
- interactions are described through the scalar σ meson for the intermediate range attraction, vector meson ω for the short range repulsion, and vector-isovector ρ for isospin dependence

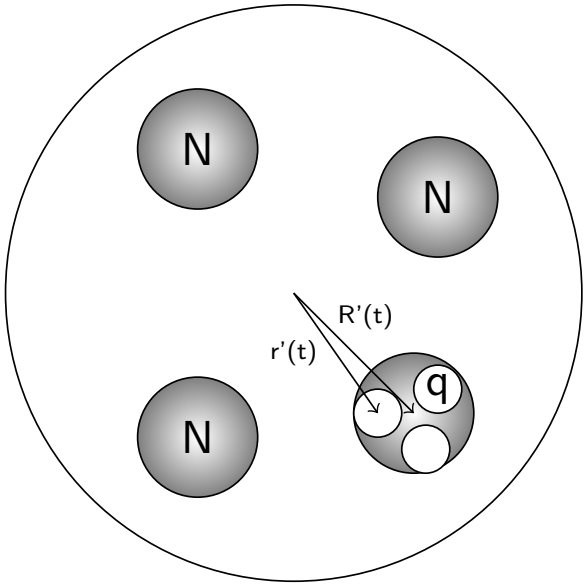

The QMC Model

Nucleon effective mass:

$$M_B^* = M_B - g_\sigma \sigma + \frac{d}{2}(g_\sigma \sigma)^2$$

The QMC Model

Nucleon effective mass:

$$M_B^* = M_B - g_\sigma \sigma + \frac{d}{2}(g_\sigma \sigma)^2$$

The *classical* total energy

$$\begin{aligned} E_{QMC} &= \sum_{i=1,\ldots} \sqrt{P_i^2 + M_i^2(\sigma(\vec{R}_i))} + g_\omega^i \omega(\vec{R}_i) + g_\rho \vec{I}_i . \vec{B}(\vec{R}_i) \\ &+ E_\sigma + E_{\omega,\rho} \end{aligned}$$

The QMC Model

To get the Hamiltonian, H_{QMC}, we eliminate the meson fields by solving the equations of motion:

$$\frac{\delta H_{QMC}}{\delta \sigma(\vec{r})} = \frac{\delta H_{QMC}}{\delta \omega(\vec{r})} = \frac{\delta H_{QMC}}{\delta B(\vec{r})} = 0$$

The QMC Model

To get the Hamiltonian, H_{QMC}, we eliminate the meson fields by solving the equations of motion:

$$\frac{\delta H_{QMC}}{\delta \sigma(\vec{r})} = \frac{\delta H_{QMC}}{\delta \omega(\vec{r})} = \frac{\delta H_{QMC}}{\delta B(\vec{r})} = 0$$

HF calculation

$$\mathcal{E}_{QMC} = \langle \Phi | H_{QMC} | \Phi \rangle$$

QMC model for finite nuclei

Densities

$$\rho_m(\vec{r}) = \sum_{i\in F_m}\sum_{\sigma}\left|\phi^i(\vec{r},\sigma,m)\right|^2, \quad \rho=\rho_p+\rho_n,$$

$$\tau_m(\vec{r}) = \sum_{i\in F_m}\sum_{\sigma}\left|\vec{\nabla}\phi^{i*}(\vec{r},\sigma,m)\right|^2, \quad \tau=\tau_p+\tau_n,$$

$$\vec{J}_m = i\sum_{i\in F_m}\sum_{\sigma\sigma'}\vec{\sigma}_{\sigma'\sigma}\times\left[\vec{\nabla}\phi^i(\vec{r},\sigma,m)\right]\phi^{i*}(\vec{r},\sigma',m),$$

$$\vec{J}=\vec{J}_p+\vec{J}_n$$

QMC model for finite nuclei

The contributions to the QMC Hamiltonian can be written as

$$H_{QMC} = H_0 + H_3 + H_{eff} + H_{fin} + H_{so} + H_\pi$$

$H_0 + H_3 \propto \rho^2$	QMC density-dependent terms
$H_{eff} \propto \rho\tau$	effective mass term
$H_{fin} \propto \nabla^2\rho$	finite size effect
$H_{so} \propto \nabla \cdot \vec{J}$	spin-orbit
H_π	single-pion exchange

QMC model for finite nuclei

The contributions to the QMC Hamiltonian can be written as

$$H_{QMC} = H_0 + H_3 + H_{eff} + H_{fin} + H_{so} + H_\pi$$

$H_0 + H_3 \propto \rho^2$	QMC density-dependent terms
$H_{eff} \propto \rho\tau$	effective mass term
$H_{fin} \propto \nabla^2\rho$	finite size effect
$H_{so} \propto \nabla \cdot \vec{J}$	spin-orbit
H_π	single-pion exchange

Model parameters: $G_\mu = \frac{g_\mu}{m_\mu^2}$ $(\mu = \sigma, \omega, \rho)$, m_σ, and λ_3

The pairing EDF

HF+BCS pairing

$$\mathcal{E}_{\mathrm{pair,q}} = \frac{1}{4} S_q(\vec{r}) \check{\rho}_q^2, \qquad \chi_{\mathrm{q}}(\vec{r}) = \sum_{\alpha \in q} u_\alpha v_\alpha |\phi_\alpha(\vec{r})|^2$$

Pairing strength

$$S_q(\vec{r}) = V_q \left[1 - \left(\frac{\rho(\vec{r})}{\rho_c} \right)^\alpha \right]$$

Volume pairing / Delta force (DF) pairing
Surface pairing / Density dependent delta interaction (DDDI)

The QMC-derived pairing EDF

Pairing potential

$$V(\vec{r}-\vec{r}') = -\left(\frac{G_\sigma}{1+d' G_\sigma \rho(\vec{r})} - G_\omega - \frac{G_\rho}{4}\right)\delta(\vec{r}-\vec{r}')$$

$$d' = d + \frac{1}{3} G_\sigma \lambda_3$$

The QMC-derived pairing EDF

Pairing potential

$$V(\vec{r}-\vec{r}') = -\left(\frac{G_\sigma}{1+d' G_\sigma \rho(\vec{r})} - G_\omega - \frac{G_\rho}{4}\right)\delta(\vec{r}-\vec{r}')$$

$$d' = d + \frac{1}{3} G_\sigma \lambda_3$$

$$V_q = G_\sigma - G_\omega - G_\rho/4, \qquad \rho_c = \frac{V_q\,(1+d' G_\sigma \rho)}{d' G_\sigma^2}, \qquad \alpha = 1$$

Coulomb and center-of-mass correction

$$\mathcal{E}_{\text{Coulomb}} = e^2 \frac{1}{2} \int d^3r d^3r' \frac{\rho_p(\vec{r})\rho_p(\vec{r}')}{|\vec{r} - \vec{r}'|} - \frac{3}{4} e^2 \left(\frac{3}{\pi}\right)^{\frac{1}{3}} \int d^3r [\rho_p]^{4/3}$$

$$\mathcal{E}_{\text{c.o.m.}} = -\langle \hat{P}_{cm}^2 \rangle / (2mA)$$

QMC versions

version	pion	$\tilde{m}_\sigma$	λ_3	full SO	$\vec{J}$	pairing
QMC-I[1]		✓				DF
QMCπ-I[2]	✓	✓				DF
QMCπ-II[8, 9]	✓	bare	✓	✓		DF
QMCπ-III[10]	✓	bare	✓	✓	✓	DDDI (QMC)

Method

Parameter optimization

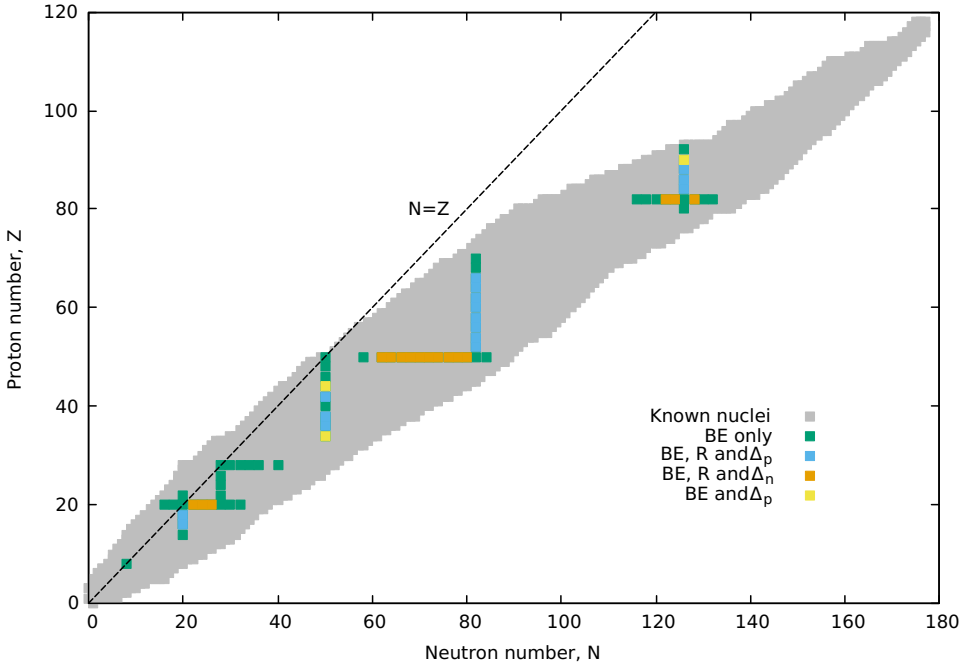

Figure 1: Doubly-magic and semi-magic nuclei included in the fit. The nuclear observables and number of data points per nucleus entering the fitting procedure are indicated.

POUNDerS algorithm

Objective function $F(\hat{\mathbf{x}})$ for minimisation

$$F(\hat{\mathbf{x}}) = \sum_{i}^{n} \sum_{j}^{o} \left(\frac{\bar{s}_{ij} - s_{ij}}{w_j} \right)^2$$

where

- n total number of nuclei
- o total number of observables
- s_{ij} experimental values
- $\bar{s}_{ij}$ fitted values
- w_j *effective* error

$w_{BE} = 1.0$ MeV
$w_{R_{ch}} = 0.02$ fm
$w_{\Delta_{p,n}} = 0.12$ MeV

Results

QMC and pairing parameters

	QMCπ-III	QMCπ-II	QMCπ-I	QMC-I
G_σ [fm^2]	9.62	9.66	11.16	11.85
G_ω [fm^2]	5.21	5.23	8.00	8.27
G_ρ [fm^2]	4.71	4.75	6.38	7.68
M_σ [MeV]	503	493	712	722
λ_3 [fm^{-1}]	0.05	0.05	-	-
V_p[MeV]	-	258	302	284
V_n[MeV]	-	237	291	326

Correlation matrix

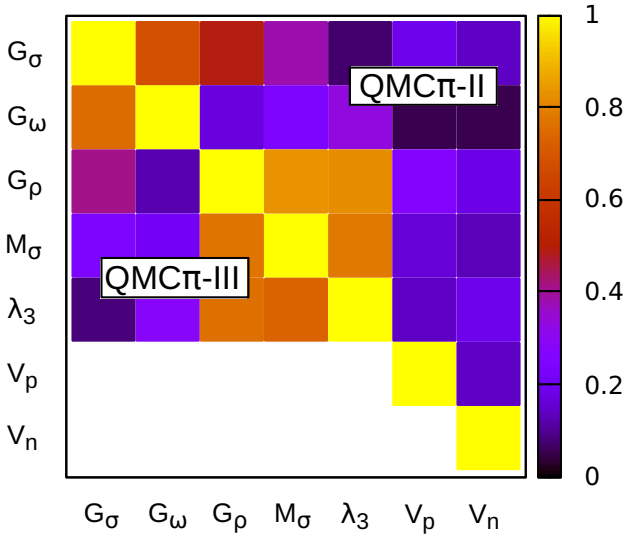

Figure 2: Correlation matrix for QMCπ-II and QMCπ-III

QMC nuclear matter properties

NMP	QMCπ-III	QMCπ-II	QMCπ-I	QMC-I	SV-min
ρ_0 (fm^{-3})	0.15	0.15	0.15	0.16	0.16
E_0 (MeV)	-15.7	-15.7	-15.8	-15.9	-15.9
a_0(MeV)	29	29	30	30	31
L_0 (MeV)	43	40	17	23	93
K_0 (MeV)	233	230	319	340	222

Even-even nuclei across the nuclear chart

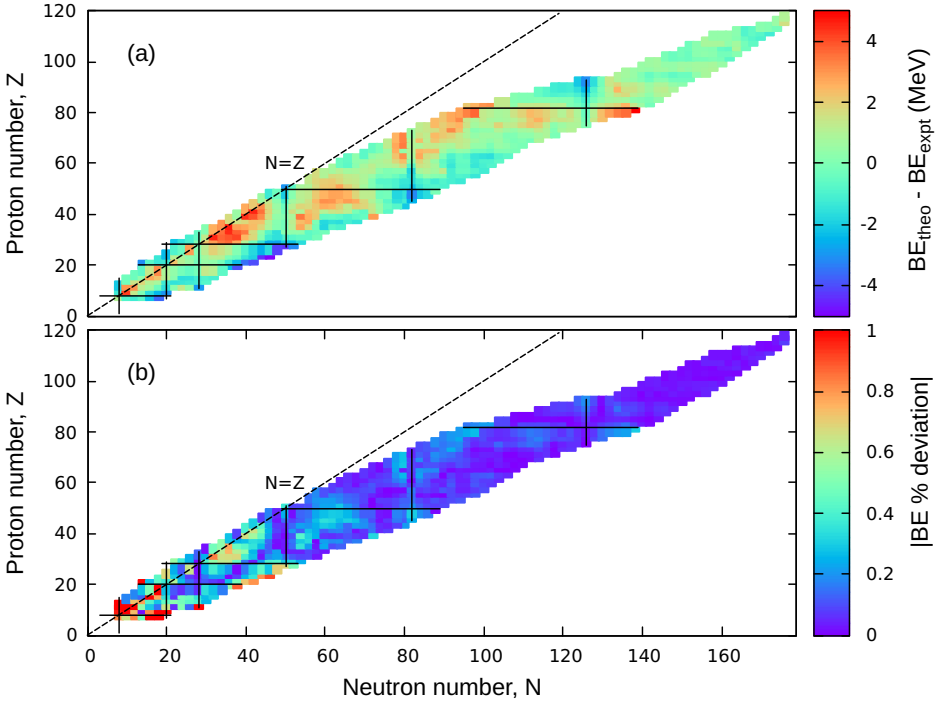

Figure 3: QMCπ-III predictions for (a) *BE* residuals and (b) absolute *BE* % deviation for even-even nuclei with known masses. Magic numbers are specified with solid lines while symmetric nuclei, $Z = N$, are shown with dashed lines.

Even-even nuclei across the nuclear chart

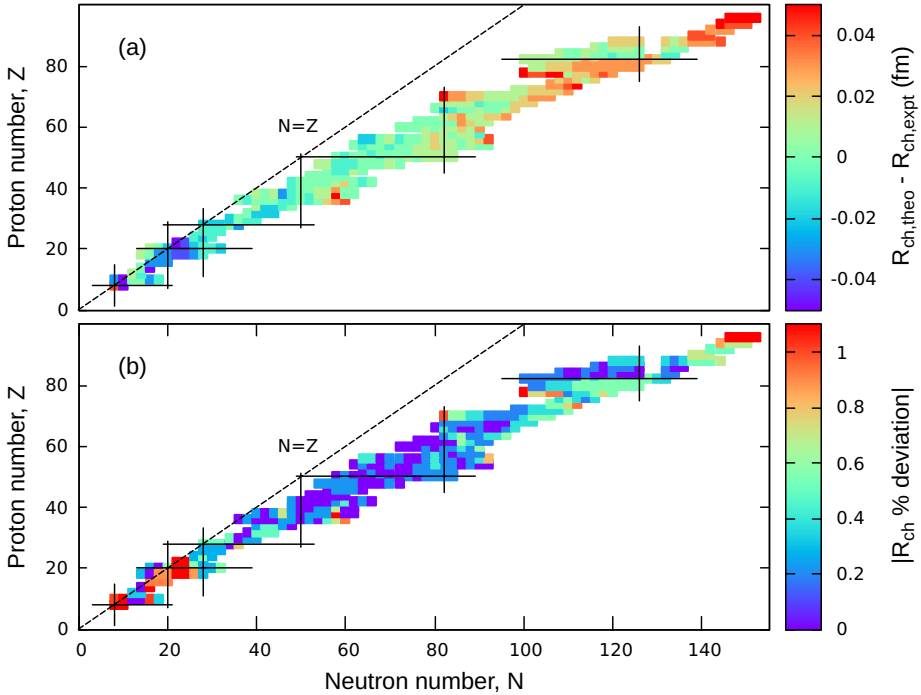

Figure 4: QMCπ-III predictions for (a) R_{ch} residuals and (b) R_{ch} % deviation for even-even nuclei with known radii. Magic numbers are specified with solid lines while symmetric nuclei, $Z = N$, are shown with dashed lines.

Even-even nuclei across the nuclear chart

Root-mean-square residuals: $\sqrt{\frac{1}{d}\sum_i^n \sum_j^o (\bar{s}_{ij} - s_{ij})^2}$

Model	BE (MeV)	R_{ch} (fm)	# of parameters
QMCπ-III	1.59	0.024	5
QMCπ-II	2.34	0.029	5+2
SV-min	3.64	0.024	11+3
UNEDF1	2.06	0.029	11+2
DD-MEδ	2.41	0.035	14+2
FRDM	0.89	-	17

Two-neutron separation energy

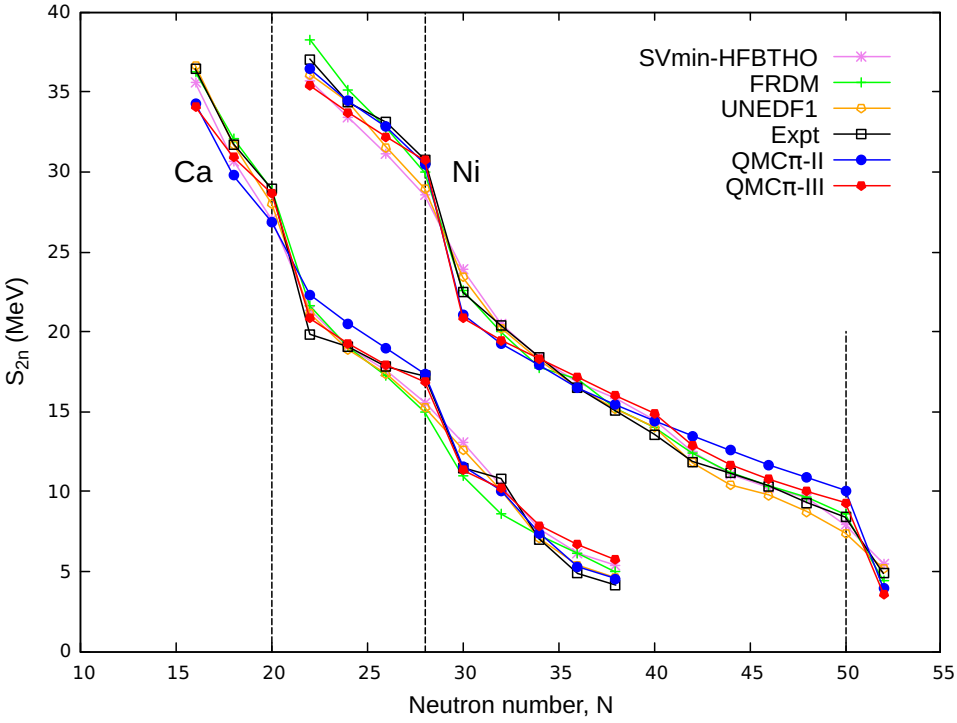

Figure 5: Two-neutron separation energies for calcium ($Z = 20$) and nickel ($Z = 28$) isotopes as a function of the neutron number.

Two-neutron shell gap

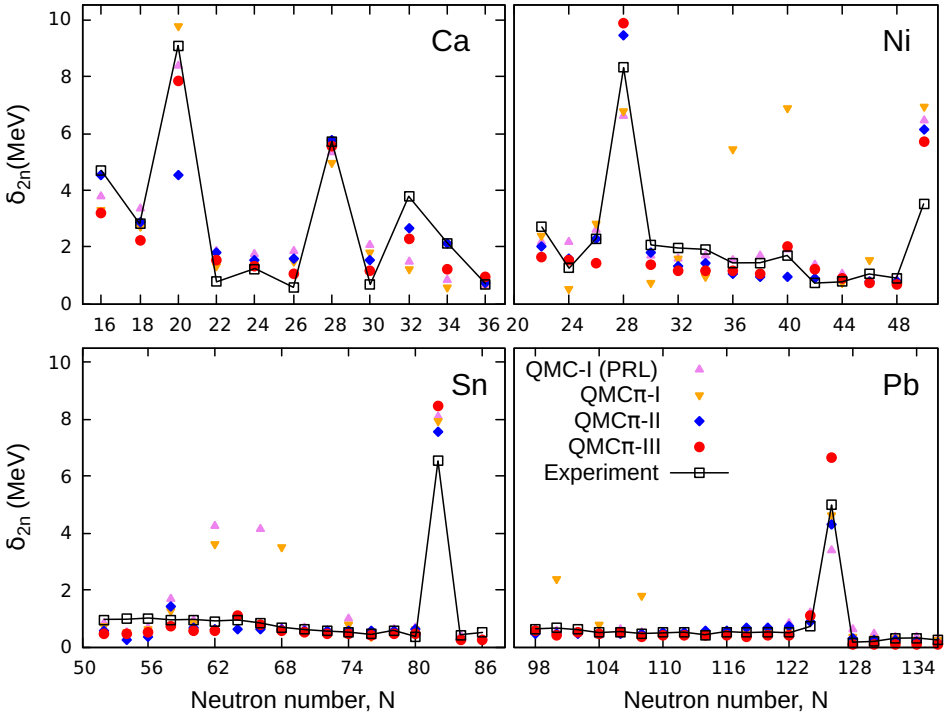

Figure 6: Two-neutron shell gaps for Ca, Ni, Sn, and Pb isotopes.

Driplines

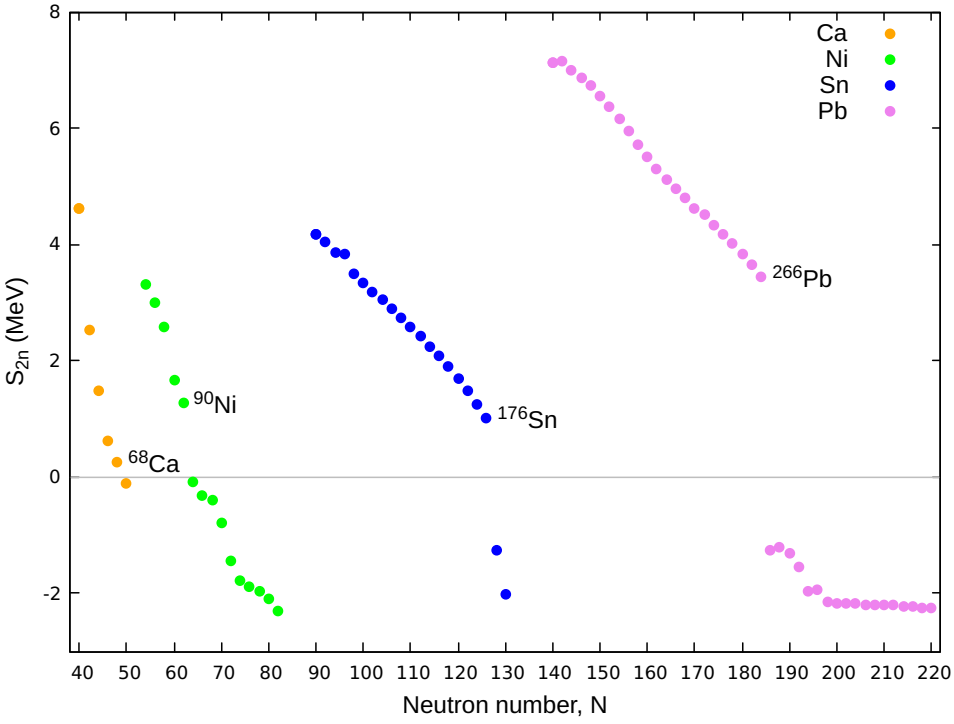

Figure 7: Neutron driplines for Ca, Ni, Sn, and Pb isotopes predicted by QMCπ-III.

Charge density plots

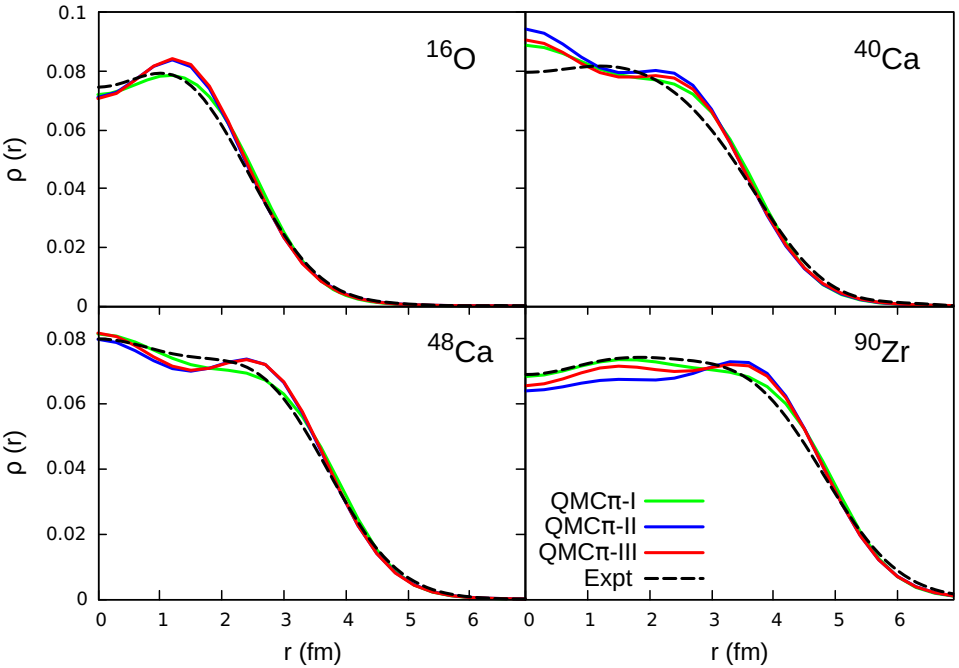

Figure 8: Charge density plots from various QMC versions compared to data from elastic scattering experiment.

Skin thickness

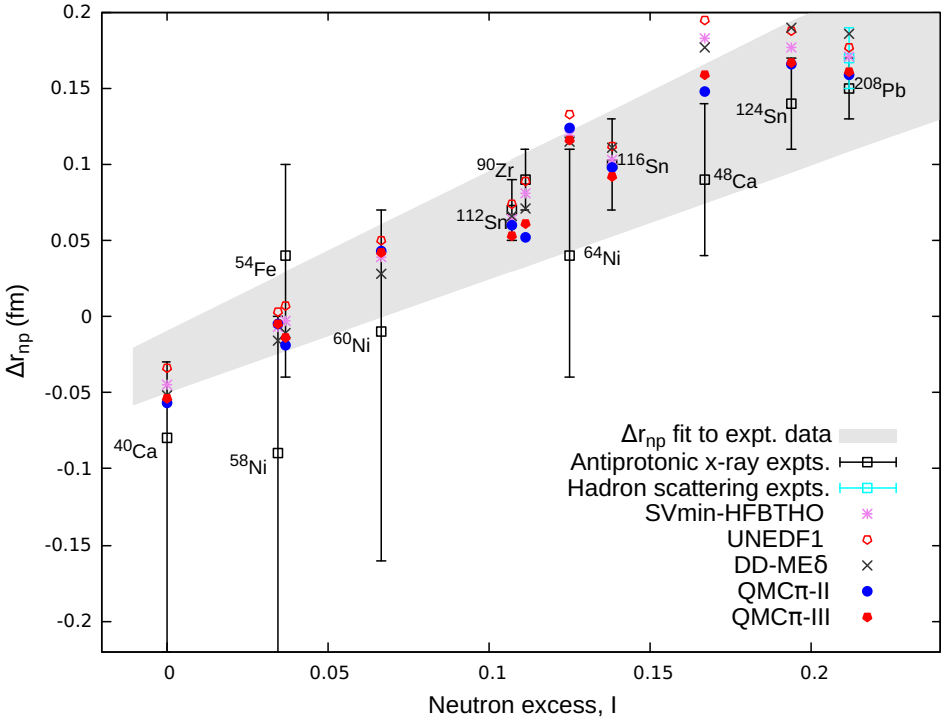

Figure 9: Skin thickness for nuclei included in the QMC fit as a function of the neutron excess.

Skin thickness and the slope of symmetry energy

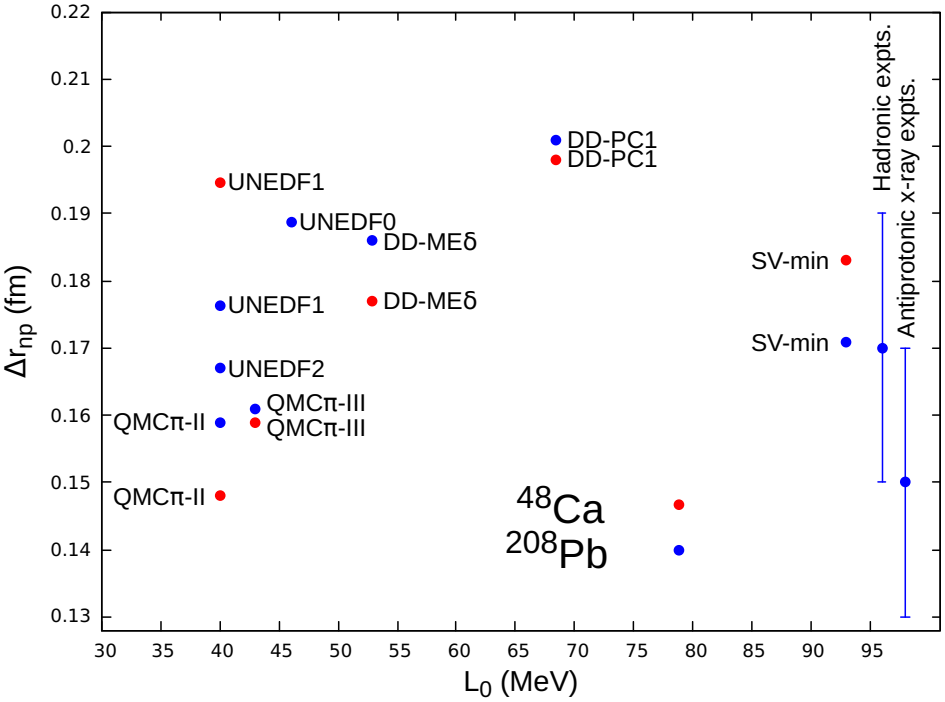

Figure 10: Neutron skin thickness plotted against L_0 for isotopes ^{48}Ca (red) and ^{208}Pb (blue) from various nuclear models.

Nuclear deformations

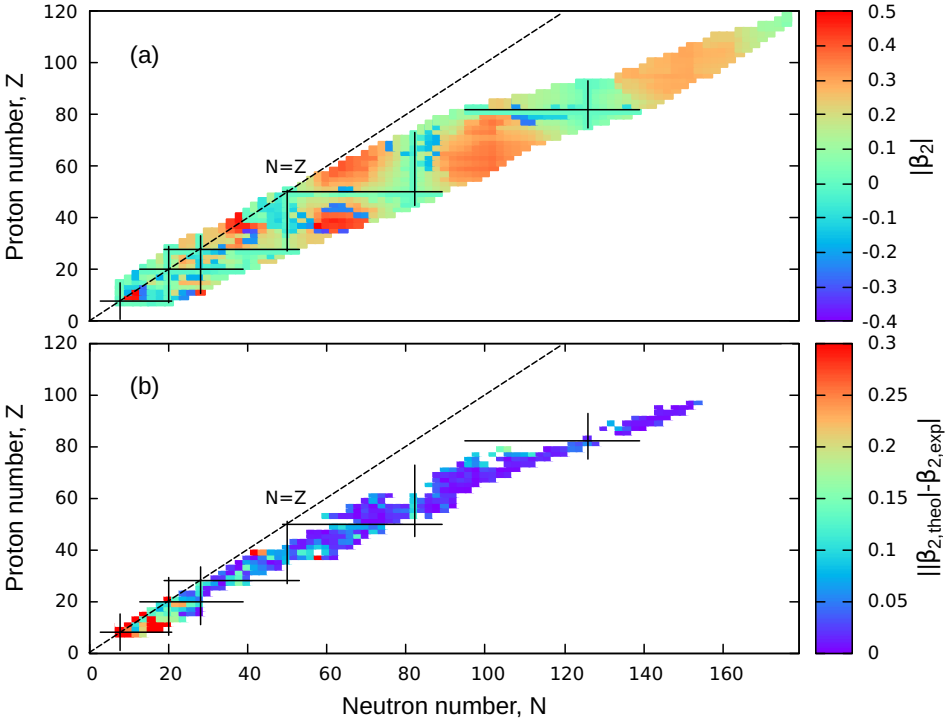

Figure 11: QMCπ-III predictions for (a) quadrupole deformation parameter, β_2, and (b) corresponding residuals upon comparison with available data [11]. Magic numbers are specified with solid lines while symmetric nuclei, $Z = N$, are shown with dashed lines.

Binding energies of even-even superheavy elements (SHE)

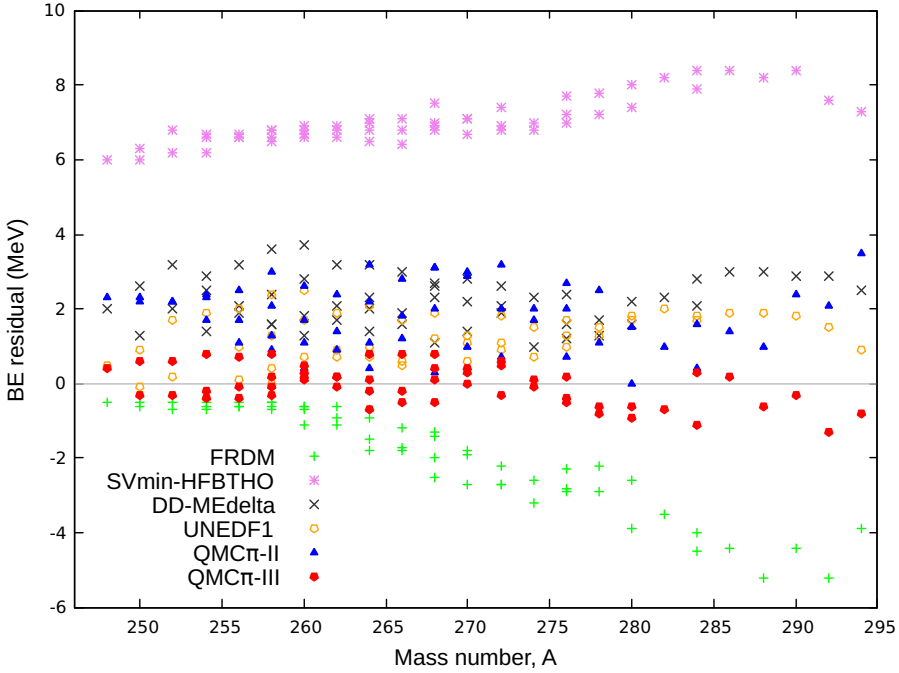

Figure 12: SHE binding energy residuals for nuclei with $Z \geq 100$ plotted against mass number A.

Subshell closures in the SHE region

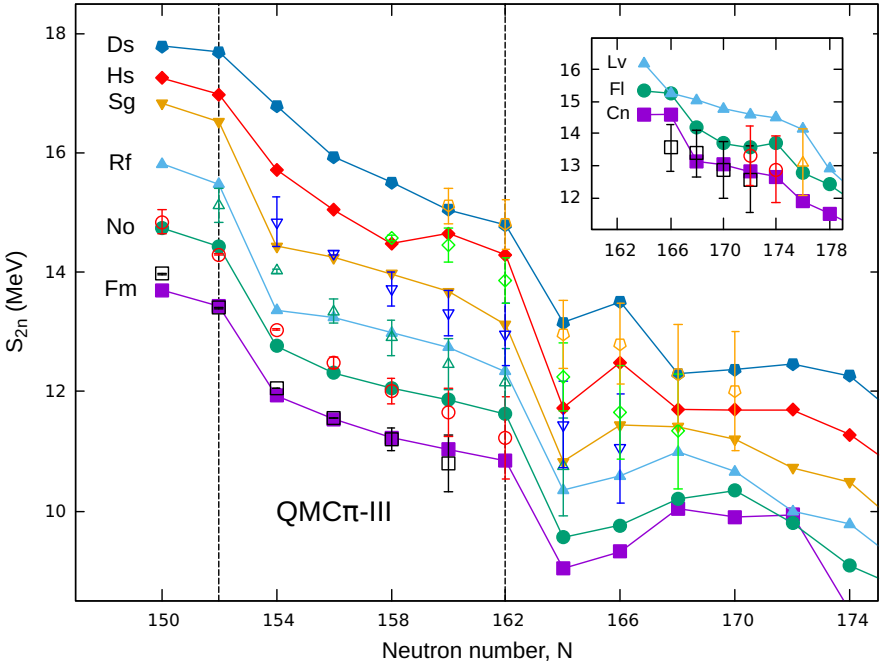

Figure 13: Two-neutron separation energies plotted against neutron number. Results from QMCπ-III are shown as filled symbols and connected by lines while experimental data and errors are shown as empty symbols with vertical errorbars. Subshell closures at $N = 152$ and $N = 162$ are indicated with dashed lines. Inset shows the S_{2n} values plotted against N for SHE with $Z \geq 112$.

Nuclear deformations in the SHE region

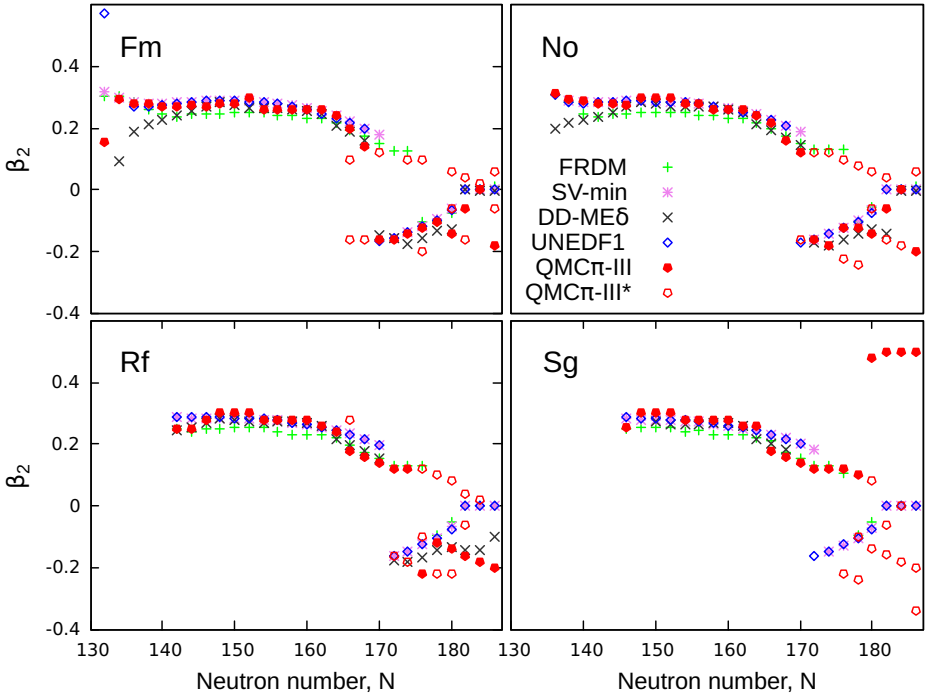

Figure 14: Comparison of deformation parameter, β_2 , values along the Fm, No, Rf, and Sg isotopic chains from several nuclear models. For QMCπ-III, the first minima are shown as filled red symbols, while the other minima, which are very close to the first, are shown as empty red symbols and labelled 'QMCπ-III*'.

Conclusion

Summary and conclusions

- Nuclear structure was described using the QMC model

Summary and conclusions

- Nuclear structure was described using the QMC model
- QMCπ-II and QMCπ-III were optimised, parameter errors and correlations were presented and the final parameter set was used to calculate various nuclear observables

Summary and conclusions

- Nuclear structure was described using the QMC model
- QMCπ-II and QMCπ-III were optimised, parameter errors and correlations were presented and the final parameter set was used to calculate various nuclear observables
- QMCπ-II and QMCπ-III produced NMPs within the acceptable range and showed considerable improvement for L_0, as well as for K_0

Summary and conclusions

- Nuclear structure was described using the QMC model
- QMCπ-II and QMCπ-III were optimised, parameter errors and correlations were presented and the final parameter set was used to calculate various nuclear observables
- QMCπ-II and QMCπ-III produced NMPs within the acceptable range and showed considerable improvement for L_0, as well as for K_0
- Ground state properties of even-even nuclei across the nuclear chart were computed and were shown to be comparable with those of other well known nuclear models

Summary and conclusions

- Nuclear structure was described using the QMC model
- QMCπ-II and QMCπ-III were optimised, parameter errors and correlations were presented and the final parameter set was used to calculate various nuclear observables
- QMCπ-II and QMCπ-III produced NMPs within the acceptable range and showed considerable improvement for L_0, as well as for K_0
- Ground state properties of even-even nuclei across the nuclear chart were computed and were shown to be comparable with those of other well known nuclear models
- Calculations were extended to other nuclear observables which had not been part of the fit

Thank you for your attention.

References I

- Stone, J. R., Guichon, P. A., & Reinhard, P. G., & Thomas, A. W. (2016). Finite nuclei in the quark-meson coupling model. *Physical Review Letters*, 092501 1-5.
- Stone, J. R., Guichon, P. A., & Thomas, A. W. (2017). Superheavy nuclei in the quark-meson coupling model. *EPJ Web Conferences*, 163 00057.
- Kortalainen, M., Lesinski, T., More, J., Nazarewicz, W., Sarich, J., Schunk, N. Stoitsov, M.V., and Wild, S. (2010). Nuclear energy density optimization. *Physical Review C*, 82 024313.
- Guichon, P.A. (1988). A possible quark mechanism for te saturation of nuclear matter. *Physical Letters B*, 5296-5299.

References II

- Thomas, A. W. (2016). QCD and a new paradigm for nuclear structure. *Heavy Ion Accelerator Symposium on Fundamental and Applied Science (HIAS 2015)* (p.01003). Canberra: EPJ Web Conferences.
- Guichon, P. A. M., Saito, K., Rodionov, E., Thomas, A. W. (1996). The role of nucleon structure in finite nuclei. *Nuclear Physics A*, 601 349-379.
- Klüpfel, P., Reinhard, P.G., Bürvenich, T.J., & Maruhn, J.A. (2009). Variations on a theme by Skyrme: A systematic study of adjustments of model parameters. *Physical Review C*, 79 034310.

References III

- Guichon, P. A. M., Stone, J. R. and Thomas, A. W. (2018). Quark-Meson-Coupling (QMC) model for finite nuclei, nuclear matter and beyond. *Prog. Part. Nucl. Phys.* 100 262–97.
- Martinez, K. L., Thomas, A. W., Stone, J. R. and Guichon, P. A. M. (2019). Parameter optimization for the latest quark-meson coupling energy-density functional. *Physical Review C*, 100 024333.
- Martinez, K. L., Thomas, A. W., Guichon, P. A. M. and Stone, J. R. (2020). Tensor and pairing interactions within the quark-meson coupling energy-density functional. *Physical Review* C 102 (2020), 034304.

References IV

S. Raman, C.W. G. Nestor Jr, and P. Tikkanen. Transition probability from the ground to the first-excited 2+ state of even-even nuclides. *Atom. Data Nucl. Data Tabl.* 78 (2001), 1–128.